doi:10.1246/cl.2012.580
Published on the web May 12, 2012

Synthesis and Growth Observation of Flower- and Spike-like Gold–Silver Nanoparticles

Keisuke Kumagai and Akito Ishida*
Department of Biomolecular Chemistry, Graduate School of Life and Environmental Sciences, Kyoto Prefectural University, 1-5 Hangi-cho, Shimogamo, Sakyo-ku, Kyoto 606-8522

(Received February 20, 2012; CL-120140; E-mail: a_ishida@kpu.ac.jp)

In this paper, we report a simple and reproducible synthesis of flower- and spike-like gold–silver (Au–Ag) nanoparticles. Reduction of aqueous solution of $AgNO_3$ and $HAuCl_4$ mixtures by L-ascorbic acid (AA) in the presence of poly(vinylpyrrolidone) (PVP) afforded the nanoparticles in a few minutes at room temperature. Stepwise trapping of the intermediate nanoparticles revealed the growth process of the petals of the flower-like nanoparticles from an initially formed nanoplate.

Au and Ag nanoparticles have attracted considerable attention as basic materials having optical properties for bottom-up nanotechnology. Because the electromagnetic field of surface plasmons is effectively localized on the sharply peaked area, it is important to develop an effective technique for the synthesis of nanoparticles with a specific shape[1,2] not only for basic research but also for practical applications such as surface-enhanced Raman scattering (SERS)[3,4] and surface-plasmon-enhanced fluorescence (SPEF).[5–7] Therefore, controlling the size and shape of metal nanoparticles is the primary focus of this research. Here we report facile synthesis and growth observation of flower- and spike-like Au–Ag nanoparticles.

The nanoparticles were typically synthesized at 25 °C. We now discuss the procedure followed for the synthesis of the above-mentioned nanoparticles. A 10 mL portion of 0.6 μM aqueous $HAuCl_4$ solution was pipetted into a polypropylene centrifugal tube, and 50 μM aqueous $AgNO_3$ solution was added to it under constant stirring in order to obtain a final concentration of 5 μM. Subsequently, 1 mL of 1 mM aqueous poly(vinylpyrrolidone) (PVP) solution followed by 0.1 mL of 0.1 mM aqueous L-ascorbic acid (AA) solution were added to the above-mentioned solution, and stirring was stopped immediately. The color of the solution changed from initial corn yellow to blue within 1 min; the resulting solution was centrifuged at 10000 rpm for 3 min and then washed twice with ultrapure water.

The Ag/Au ratio of the prepared nanoparticles was determined to be 14.5 by the inductively coupled plasma (ICP) analysis; this value was rather different from the ratio of the starting solution (8.3), thereby suggesting incomplete reduction of Au^{3+}. To observe the morphology of the nanoparticles, a hydrophilic amino-coated (MAS® coated) glass slide was used as a substrate, and the nanoparticles were immobilized by dipping the substrate in the above-prepared solution for 2 h. The substrate with the immobilized nanoparticles was washed with ultrapure water and dried with clean air. A MAS-coated surface facilitates good affinity between the biological samples and the negatively charged gold colloids owing to its strong hydrophilicity and adhesion properties; this affinity is much better than that achieved by a conventional amino-terminated glass substrate coated with aminopropyltrimethoxysilane (APTMS)[8] or poly-L-lysine (PLL). The SEM (scanning electron microscopy) observations revealed that the synthesized nanoparticles are characterized by a flower-like structure (Figure 1d). Because the nanoparticles were obtained as an alloy, the following reactions are assumed to be responsible for the formation of the nanoparticles.

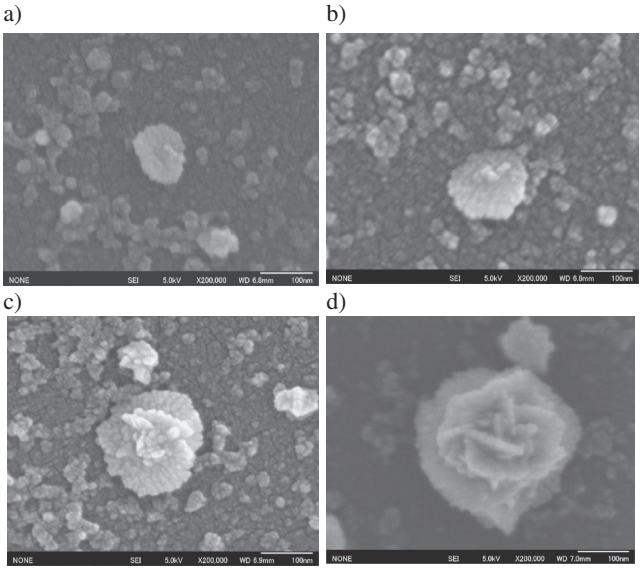

Figure 1. SEM images of the flower-like particles isolated at the different reaction times (approximate) on a MAS-coated glass: a) $t = 0$ s, b) $t = 40$ s, c) $t = 80$ s, and d) after the reaction completed $t = 8$ h. All scale bars are 100 nm.

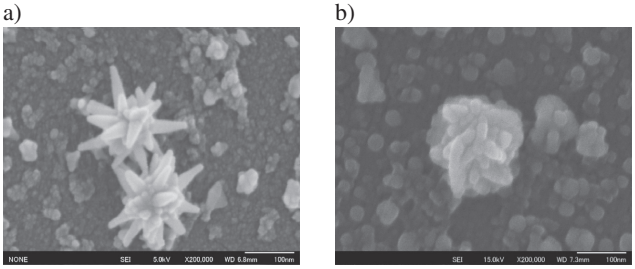

Figure 2. SEM images of the spike-like particles on a MAS-coated glass prepared a) in the absence of PVP (50 μL of 0.1 mM AA) and b) in the presence 0.1 mL of 0.5 mM PVP. Scale bars are 100 nm.

$$2Ag^+ + C_6H_8O_6 \rightarrow 2Ag + C_6H_6O_6 + 2H^+ \quad (1)$$

$$2Au^{3+} + 3C_6H_8O_6 \rightarrow 2Au + 3C_6H_6O_6 + 6H^+ \quad (2)$$

Spike- or flower-like nanoparticles have been synthesized even in the absence of PVP (Figure 2),[9] but these nanoparticles have much lower concentrations of $AgNO_3$ and $HAuCl_4$ than the reported typical concentrations.[10] This fact shows that PVP is indispensable for the synthesis of flower-like nanoparticles. From the morphological observations, which were made for the

synthesis of the nanoparticles in the presence of PVP with constant concentration, it was found that the molar ratios of $AgNO_3$ and $HAuCl_4$ relative to PVP play important roles in determining the shape and size of the nanoparticles, respectively. For example, nanocubes were synthesized when the Ag/Au ratio of the starting solution was 16.6. In contrast, nanoplates were selectively synthesized when the Ag/Au ratio of the starting solution was 4.2. On reversing the sequence of addition of AA and $HAuCl_4$ to the reaction solution, i.e., when the addition of AA was followed by the addition of $HAuCl_4$, large spherical nanoparticles were synthesized instead of the flower-like nanoparticles.[10] The nanoparticles were believed to be formed by the aggregation of primary small nanoparticles.

In order to study the growth process of the nanoparticles, we attempted to trap the intermediate nanoparticles by carrying out rapid centrifugation. The intermediate particles were effectively isolated by the rapid centrifugation (2 min) of the solution[11] i.e., at 0, 40, 80, and 120 s intervals after the addition of AA. The SEM images in Figures 1a–1c show the intermediate nanoparticles isolated at 0, 40, and 80 s, respectively, and the SEM image in Figure 1d shows the synthesized flower-like nanoparticles after the completion of the reaction. In the initial stage of the reaction ($t = 0$ s), nanoplates having a short tip at the center of each nanoparticle were formed (Figure 1a). In the next stage ($t = 40$ s), both the size of the nanoplates and the number of tips increased (Figure 1b). With further increase in the reaction time ($t = 80$ s), the nanoplates continued to grow and new secondary plates were formed at the center of the base nanoplate (Figure 1c). After the completion of the reaction, the nanoparticles transformed into carnation-like structures with their petals having a thickness of ca. 4 nm and extending radially from the center of the primary nanoplate. Careful observation of the SEM images of the nanoparticles isolated at 40 s strongly suggested that the new petals grew only from the primary plate by displacing the petals formed previously. The growth process of the nanoparticles is expected to bring about remarkable changes in their plasmonic property. The absorption spectra of the isolated nanoparticles are summarized in Figure 3. In the initial stages of the reaction ($t = 0$ s), a relatively broad absorption spectrum with a maximum at around 523 nm was observed (Table 1). The maximum can possibly be attributable to the Au nanoparticles and/or nanoplates that were formed initially. It should be noted that no absorption band was observed at 410 nm, indicating that the independent reduction of Ag^+ did not occur effectively. In the next stage ($t = 40$ s), a shoulder was observed around 650 nm with a maximum at 538 nm.

This change may be consistent with the growth of the petals on the primary nanoplate. With a further increase in the reaction time ($t = 80$ s), the plasmonic absorption maximum of Au nanoparticles disappeared and rather broad absorption spectra with a gradually red-shifted maximum at around 560–580 nm were observed. These broad absorption spectra may be attributed to the summation of the individual plasmonic absorption bands of the all flower-like particles. Although the simultaneously measured dynamic laser scattering (DLS) data indicates the growth of the nanoparticles, it only provides their diameters with globular approximation.

The following three factors are assumed to be responsible for the synthesis of the flower-like nanoparticles: (1) change in the preferentially reduced facets with AA, (2) change in the composition of the nanoparticles depending on the ratio of Ag/Au, and (3) stabilization of the spike ends of the growing nanoparticles by PVP. Each of these factors is discussed subsequently. It is reported that direct reduction of Ag^+ by AA cannot occur in acidic conditions in the presence of PVP;[12] however, AA can reduce Au^{3+} directly because the reduction potentials for $AuCl_4/Au$ and $C_6H_6O_6/C_6O_8H_6$ are +0.99 (aqueous)[13] and +0.17 V (pH 3.4),[12] respectively. Given the fact that our reactions were also carried out at pH 3.80 in the presence of PVP, direct reduction of Ag^+ by AA did not occur. Thus, reduction of Au^+ by AA should occur first to form initial nuclei, on which the following coreduction of Ag^+ and Au^{3+} may induce the growth of nanoparticles. He et al. reported the selective preparation of a Au–Ag nanobox using $HAuCl_4$, $AgNO_3$, and AA.[10] Their study focused on the effect of Au and Ag concentrations in the solution and the rate of displacement of Ag with respect to the residual Au^{3+} in the solution. It was reported that under the condition of fixed Au concentration of 0.1 mM, star-like nanoparticles, nanoboxes, and broken nanoboxes were synthesized with Ag/Au ratios of 0.2, 1, and 1.5, respectively, whereas under a fixed Ag/Au ratio of 1 and Au concentrations higher than 0.25 mM, star-like nanostructures were selectively synthesized. These alloys are known to have a large electrochemical driving force; therefore, they aid in the reduction of Au^{3+} via the displacement reaction. As a result, Ag grows faster at higher Ag/Au ratios, leading to the formation of nanoparticles with a higher Ag content. This displacement reaction contributed in a similar manner to the present reactions that were carried out under a very high Ag/Au ratio of 8.3. It has

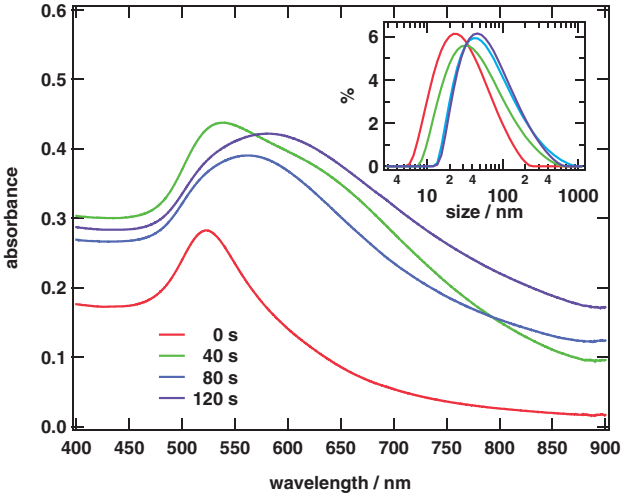

Figure 3. The change in the absorption spectra and the DLS size distribution (inset) of the intermediate particles observed by centrifugation of the solution 0 (red), 40 (green), 80 (blue), and 120 s (purple) after the addition of AA.

Table 1. Change in the absorption maxima of the plasmonic bands and Ag/Au ratios of the flower-like nanoparticles isolated by rapid centrifugation

Reaction time/s	λ_{max}/nm	Ag/Au[a]
0	523	0.28
40	538	0.35
80	562	2.1
After the reaction	625	14.5

[a]The Ag/Au ratios were determined by ICP analysis.

been reported that in the presence of PVP, the reduction of Ag becomes slow and that the growth of the nanoparticles becomes anisotropic because PVP is more preferentially adsorbed on specific crystal planes, i.e., it is adsorbed more on Ag{100} facets than on Ag{111} facets.[14] Thus, the Ag{111} facets remain accessible to the incoming Ag atoms whereas the side surface at the Ag{100} facets is completely passivated by PVP. As a result, nanorods are selectively formed.[15] On the other hand, in the case of Au nanoparticles, PVP interacts more strongly with the Au{111} facets than with the Au{100} facets. Therefore, Au{111} facets remain accessible to the incoming Au atoms whereas the top surface at the Au{100} facets is passivated by PVP. As a result, nanoplates are selectively formed. In the present study, although Au^{3+} coexists with Ag in the presence of PVP, the nanoplates are initially formed as indicated by the SEM images. In the presence of excessive amount of PVP such as 0.1 mM, aggregated nanoparticles with complex shapes were obtained instead of the flower-like nanoparticles. These facts suggest that PVP molecules are more preferably adsorbed on the Au{111} than on the Ag{100} facets and that there is an effective concentration range of PVP within which the Au{111} and the Ag{100} are suitably passivated for the selective formation of flower-like nanoparticles.

On the basis of the above-mentioned results, we now propose the growth mechanism of the nanoparticles synthesized in this study. In the absence of PVP, Au^{3+} is more rapidly reduced than Ag^{+} by AA, leading to the formation of nuclei with a spherical shape. Therefore, most of the Au^{3+} could possibly be consumed after the formation of the initial nuclei, and the successive reduction of the residual Ag^{+} leads to the growth of the tips on the surfaces of the nuclei. As a result, spike-like nanoparticles are formed (Figure 2a). On the other hand, in the presence of 1 mM PVP, the reaction rate of Au^{3+} was reduced owing to the influence of PVP, and the initial nuclei grew to form nanoplates (Figure 1a). The insufficiency of PVP resulted in the formation of the nanoparticles with blunt spikes (Figure 2b).

The SEM images suggested that the petals initially grew upward from the center and then grew sequentially along the central axis of the initially formed nanoplates. Now, we consider the growth process of the petals. The Ag/Au ratio of 14.5 determined by the ICP analysis, which was performed after the formation of the nanoplates, suggests that sufficient amount of Au^{3+} still remains in the solution for the petal growth. Once the nanoplates have been formed, the unconsumed Au^{3+} and AA in the solution should be mainly used for the growth of the rim of the nanoplates and for the formation of the petals and not for the formation of the initial nuclei. This process is supported by the absorption spectral change indicating that the plasmonic absorption band at 520 nm was no longer observed after the formation of the nanoplates having broad absorption band of around 650 nm. Thus, the growth rate of the nanoplates and petals should be higher than that of the initial nuclei. As shown in the SEM image, the reaction without Au^{3+} selectively afforded spike-like Ag nanostructures. This selective growth of the tips of the nanoparticles is attributed to the protection of the side facets of the spikes by PVP. The thickness of the petals of the Au–Ag nanoparticles is remarkably less than the diameter of the Ag spikes.

These findings may suggest that Au induced the breakage of the PVP protection layer at the side facet of the growing Ag spikes and that the rapid deposition of Au and Ag between the small spikes resulted in formation of the petals before the growth of the Ag spikes. It has been reported that at low Au/Ag ratios (ca. 0.08–0.17), a thin layer of Au is deposited on the edges of the Ag nanoprisms without any structural damage typically associated with galvanic replacement. In this case, since the ratio of Au/Ag is 0.12, the galvanic replacement reaction of Ag by Au^{3+} as well as its reduction by AA may contribute to the rapid deposition of Au. The gradual increase in the Ag/Au ratio with increasing the reaction time (Table 1) suggests the continuous deposition of Au together with Ag.

Unfortunately, the distribution of Au and Ag on the petals could not be determined by electron probe microanalysis (EPMA) owing to the limitation of the spatial resolution. The flower-like nanoparticles could have acquired the shape of an opening flower by repeating the above-mentioned process.

In conclusion, synthesis of flower-like Au–Ag nanoparticles by using AA and PVP has been demonstrated. The sequential SEM images indicated that the flower-like nanoparticles have been grown through the stepwise growth of the petal-like thin plates on the initially formed nanoplates. Furthermore, the tip lengths of the spike-like nanoparticles (and thus their optical properties) could be readily controlled by changing the volume of AA added into the reaction solution. The surface plasmon resonance (SPR) peaks could be readily tuned to the near-infrared region to match the transparent window of the biological samples. It is expected that such flower- and spike-like nanoparticles may find use in controlled optical sensing and SERS applications.

The authors acknowledge Dr. Hiroshi Kitagaki (Kyoto Prefectural Technology Center for Small and Medium Enterprises), Prof. Junta Yanai (Kyoto Prefectural University), and Mr. Tatsuo Igushi (Horiba Ltd.) for supporting the SEM, ICP, and DLS measurements, respectively. This work was supported by KAKENHI (Grant-in-Aid for Scientific Research) on Scientific Research (C) (No. 20510117) from MEXT.

References and Notes

1 S. Chen, Z. L. Wang, J. Ballato, S. H. Foulger, D. L. Carroll, *J. Am. Chem. Soc.* **2003**, *125*, 16186.
2 D. Aherne, D. M. Ledwith, J. M. Kelly, *Synthesis of Anisotropic Noble Metal Nanoparticles* in *Metal-Enhanced Fluorescence*, ed. by C. D. Geddes, John Wiley & Sons, Inc., Hoboken, New Jersey, **2010**, p. 295.
3 B. K. Jena, C. R. Raj, *Chem. Mater.* **2008**, *20*, 3546.
4 J. Xie, Q. Zhang, J. Y. Lee, D. I. C. Wang, *ACS Nano* **2008**, *2*, 2473.
5 T. Nakamura, S. Hayashi, *Jpn. J. Appl. Phys.* **2005**, *44*, 6833.
6 Y. Fu, J. Zhang, J. R. Lakowicz, *J. Fluoresc.* **2007**, *17*, 811.
7 K. Aslan, C. D. Geddes, *Metal-Enhanced Fluorescence: Progress towards a Unified Plasmon-Fluorophore Description* in *Metal-Enhanced Fluorescence*, ed. by C. D. Geddes, John Wiley & Sons, Inc., Hoboken, New Jersey, **2010**, p. 1.
8 A. Ishida, K. Kumagai, *Chem. Lett.* **2009**, *38*, 144.
9 Supporting Information is available electronically on the CSJ-Journal Web site, http://www.csj.jp/journals/chem-lett/index.html.
10 W. He, X. Wu, J. Liu, X. Hu, K. Zhang, S. Hou, W. Zhou, S. Xie, *Chem. Mater.* **2010**, *22*, 2988.
11 Y. Wang, P. H. C. Camargo, S. E. Skrabalak, H. Gu, Y. Xia, *Langmuir* **2008**, *24*, 12042.
12 L. Lu, A. Kobayashi, K. Tawa, Y. Ozaki, *Chem. Mater.* **2006**, *18*, 4894.
13 Y. Jin, S. Dong, *J. Phys. Chem. B* **2003**, *107*, 12902.
14 J. Chen, B. J. Wiley, Y. Xia, *Langmuir* **2007**, *23*, 4120.
15 F. Kim, S. Connor, H. Song, T. Kuykendall, P. Yang, *Angew. Chem., Int. Ed.* **2004**, *43*, 3673.

